Structural Eng./Earthquake Eng. Vol. 9, No. 1, 21s-32s, April 1992
Japan Society of Civil Engineers (Proc. of JSCE No. 446/ I -19)

IMPEDANCE MATRICES FOR AXIAL SYMMETRIC FOUNDATIONS ON LAYERED MEDIA

Gin-Show LIOU* and George C. LEE**

A procedure to generate the impedance matrix of foundation resting on an elastic layered half-space medium is proposed. The prescribed harmonic loadings due to the foundation are decomposed into an infinite Fourier series with respect to the azimuth. For each Fourier component, the analytic solution is obtained by solving the differential equations of wave propagation satisfying the prescribed boundary conditions, and the stress and the displacement continuity conditions at the horizontal interfaces in the layered system. Using this analytic solution, the impedance matrix is obtained by applying the variational principle and the reciprocal theorem with the assumption that the interaction stresses between the foundation and the soil is piecewise linear in the radial direction of cylindrical coordinates. An example of a two-layer system is often presented.

Keywords : *axial symmetry, layered medium, impedance*

1. INTRODUCTION

In recent years, the effect of wave scattering in soil medium caused by the existence of structure has attracted much attention because of the construction of massive structures, such as nuclear power plants, offshore oil drilling platforms and arch dams, in seismic areas. To perform the soil-structure interaction analysis, the substructuring technique is often employed. In such application, the surrounding soil medium of the structural foundation is represented by an impedance matrix which can then be combined into the total stiffness matrix of the structural finite element model. Therefore, how to generate the impedance matrix is an important step for soil-structure interaction analyses.

Several numerical methods with specific assumptions can be used to generate the impedance matrix, e.g. hybrid modelling method and boundary element method. In the hybrid modelling method, the soil medium is divided into a far-field and a near-field. The far-field is modelled by either an analytic or a semi-analytic method and the near-field is typically modelled by the finite element method. Then the displacement and the stress continuities are invoked to combine the far-field and the near-field models in order to generate the impedance matrix for the foundation[1),2)]. In the boundary element method, Green's function is used as fundamental solution in the soil medium and the formulation of weighted residual is employed to minimize the error caused by the discrepancy between the Green's function and the finite element solution of structural foundation at the interface of the soil medium and the foundation[3),4)]. The analytic approach presented in this paper is an effective and efficient method to generate the impedance matrix for surface foundation when compared with other available numerical methods.

There are analytic procedures available for generating impedance functions for rigid surface foundations. For vertical vibration of rigid circular plate, Lysmer employed the analytic solution for constant normal ring-traction on half-space medium to generate vertical compliance function for the rigid circular plate[5)]. Ruco and Westmann have obtain the compliance functions for rotational, vertical, horizontal and rocking vibrations of rigid circular plate on half-space medium by reducing Fredholm integral equation to algebraic equations using finite difference method[6)]. Luco also applied the same methodology to solve the compliance functions for rigid circular foundation on layered medium and layered viscoelastic medium[7),8)]. Wong and Luco have applied the idea similar to Lysmer's to generate the compliance for rigid foundations with arbitary shape on half-space medium[9)]. However, in the above mentioned analytic procedure, a relaxed boundary condition has been assumed, which ignores the contact shear stress between the foundation and the soil medium for the vertical and the rocking vibrations of the foundation and ignores the contact normal stess for the horizontal vibration.

This paper presents a systematic procedure to generate impedance matrices for foundations on layered half-space media without making the

* Associate Professor, Depatment of Civil Engineering, National Chiao-Tung University (Hsin-Chu, Taiwan 30049)
** Professor and Dean, School of Engineering, 412 Bonner Hall, SUNY Buffalo, NY 14260

assumption of relaxed boundary condition. Therefore, impedance matrices for flexible foundations can also be generated. Based on a technique of decomposing arbitarily prescribed boundary condition developed in Ref.10), the analytic solution for arbitary dynamic loadings applied on the surface of layered medium is presented. According to Ref.[10], the arbitarily prescribed displacements or tractions on layered medium can be expressed in terms of an infinite series of Fourier components with respect to the azimuth. Each Fourier component can then be decomposed into series of Bessel functions with respect to the radial direction of cylindrical coordinates. They can easily be shown to satisfy the general solution of the differential equations of wave propagation in layered medium[10].

In order to use this analytic solution to generate impedance matrix, the interaction stresses between foundation and surrounding soil is assumed to be piecewise linear in the r-direction of cylindrical coordinates. Enforcing the compatibility condition of the foundation and the soil medium, the impedance matrix for each Fourier component is formulated using the variational principle and the reciprocal theorem.

Numerical results for a rigid massless circular plate rigidly attached to the surface of a soil layer underlain by a half-space soil medium are presented to demonstrate the proposed approach. The numerical results include torsional, vertical, rocking and horizontal impedances. The coupling impedance for rocking and horizontal excitations is also presented. Since the behaviors of the impedance funcions change dramatically with the soil properties of the half-space layer in the two-layer system, the impedance functions for different combinations of soil properties are compared in order to show the significance of layered stratum.

2. ANALYTIC SOLUTION FOR DYNAMIC LOADING ON LAYERED MEDIUM

The analytic solution for dynamic loading on layered medium will now be described. First of all, the general solution of the differential equations of wave propagation is independently found for each layer in the layered medium. The displacement and the stress continuity conditions at the horizontal interfaces in the layered system are then imposed in order to express the displacement and the stress fields in terms of the prescribed dynamic loadings. Since the displacements at the contact area with the structural foundation are only of interest in the soil-structure interaction analysis, the following discussions are focused on the relations between the stress and the displacement components on the horizontal planes.

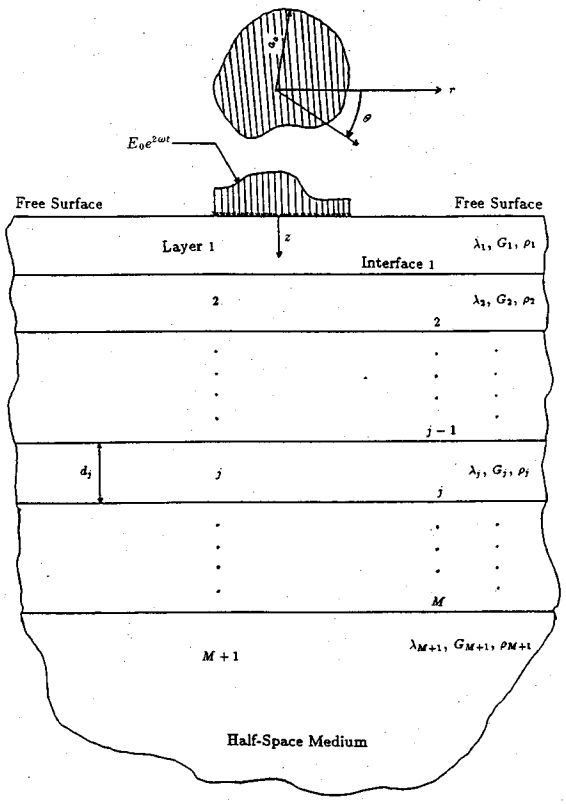

Fig.1 Dynamic Loading on Layered Half-Space Medium.

The dynamic harmonic loadings applied on the surface of a layered half-space medium is shown in **Fig.1**. In this figure, the dynamic loadings are applied at the shaded area and the complementary area on the surface is traction free. The dynamic loadings can be decomposed into an infinite series of Fourier components with respect to the azimuth as follows :

$$\begin{Bmatrix} \bar{\tau}_{rz}(r,\theta) \\ \bar{\sigma}_{zz}(r,\theta) \\ \bar{\tau}_{\theta z}(r,\theta) \end{Bmatrix} e^{i\omega t} = \sum_{n=0}^{\infty} \begin{Bmatrix} \bar{\tau}^n_{rz}(r) & \begin{pmatrix} \cos n\theta \\ \sin n\theta \end{pmatrix} \\ \bar{\sigma}^n_{zz}(r) & \begin{pmatrix} \cos n\theta \\ \sin n\theta \end{pmatrix} \\ \bar{\tau}^n_{\theta z}(r) & \begin{pmatrix} -\sin n\theta \\ \cos n\theta \end{pmatrix} \end{Bmatrix} e^{i\omega t}, \quad 0 \le r \le a_0 \cdots\cdots\cdots\cdots (1)$$

Where superscript n denotes the n^{th} Fourier component in the series, ω is the frequency and a_0 is the distance from the origin of cylindrical coordinates to the farthest point on the shaded area. Since the time variation $e^{i\omega t}$ will appear on both sides of all the equations in the following

mathematical manipulations, it is omitted in the subsequent equations. Through the principle of superposition, it is sufficient to describe the solution procedure by considering only one particular Fourier component (n^{th} component) in Eq.(1) as the prescribed traction on the area $0 \leq r \leq a_0$. In addition, the superscript n denoting the n^{th} Fourier component is omitted for convenience in the formulations that follow.

Now, considering a particular layer j in the total system shown in **Fig.1**, the general differential equations of wave propagation in the layer with harmonic excitation can be written as follows :

$$-\omega^2\rho_j u_r=(\lambda_j+2G_j)\frac{\partial\Delta}{\partial r}-\frac{2G_j}{r}\frac{\partial w_r}{\partial\theta}+2G_j\frac{\partial w_\theta}{\partial z}$$

$$-\omega^2\rho_j u_z=(\lambda_j+2G_j)\frac{\partial\Delta}{\partial z}-\frac{2G_j}{r}\frac{\partial(rw_\theta)}{\partial r}+\frac{2G_j}{r}\frac{\partial w_r}{\partial\theta}$$

$$-\omega^2\rho_j u_\theta=\frac{(\lambda_j+2G_j)}{r}\frac{\partial\Delta}{\partial\theta}-2G_j\frac{\partial w_r}{\partial z}+2G_j\frac{\partial w_z}{\partial r} \quad \cdots\cdots(2)$$

where subscript j denotes the j^{th} layer, λ_j and G_j are the Lame's constants, ρ_j is the mass density of the soil, ω is the frequency, Δ is the dilatation, and w_r, w_z and w_θ are the rotations.

To solve Eqs. (2), one can use the technique developed by Sezawa to separate the dilatational waves from the rotational waves and then use the technique of separation of variables to solve the independent differential equations for the dilatational waves and the rotational waves[11]. After combining the solutions for the dilatational and the rotational waves, the general solution of Eqs. (2) for the n^{th} Fourier component can be expressed in the matrix form as follows :

$$\begin{Bmatrix} u_r(r,z) & \begin{pmatrix}\cos n\theta\\ \sin n\theta\end{pmatrix} \\ u_z(r,z) & \begin{pmatrix}\cos n\theta\\ \sin n\theta\end{pmatrix} \\ u_\theta(r,z) & \begin{pmatrix}-\sin n\theta\\ \cos n\theta\end{pmatrix} \end{Bmatrix} = \begin{bmatrix} \begin{pmatrix}\cos n\theta\\ \sin n\theta\end{pmatrix} & 0 & 0 \\ 0 & \begin{pmatrix}\cos n\theta\\ \sin n\theta\end{pmatrix} & 0 \\ 0 & 0 & \begin{pmatrix}-\sin n\theta\\ \cos n\theta\end{pmatrix} \end{bmatrix} \boldsymbol{J\kappa_1 eA} \quad \cdots\cdots(3)$$

or

$$\boldsymbol{Lu=LJ\kappa_1 eA}$$

where

$$J=\begin{bmatrix} J_n'(kr) & 0 & \frac{n}{r}J_n(kr) \\ 0 & kJ_n(kr) & 0 \\ \frac{n}{r}J_n(kr) & 0 & Jh(kr) \end{bmatrix}, \quad \cdots\cdots(4)$$

matrix κ_1 is defined by Eq. (A-1) in Appendix, vector $A=(A_1, B_1, C_1, A_2, B_2, C_2)^T$ are the unknown coefficients determined from the boundary conditions at the upper and the lower interfaces of the layer, matrix $e = diag\ (e^{-\nu_j z}, e^{-\nu_j' z}, e^{-\nu_j z}, e^{\nu_j z}, e^{\nu_j' z}, e^{\nu_j z})$, $\nu_j = \sqrt{k^2-\frac{\omega^2}{c_{pj}^2}}$, $\nu_j' = \sqrt{k^2-\frac{\omega^2}{c_{gj}^2}}$, c_{pj} and c_{gj} are the compressional and the shear wave velocities in the layer (j^{th} layer), k is the wave number in the horizontal direction, $J_n(kr)$ is the first kind of Bessel founction of order n, and $J_n'(kr)=\frac{dJ_n(kr)}{dr}$.

The stress field in the layer can be obtained by differentiating the displacement field of Eq.(3) with respect to the corresponding variables r, z and θ, and then multiplying it with the constitutive matrix of elasticity. The stress components on the horizontal plane, with the azimuthal variation matrix L shown in Eq.(3) factored out, can then be expressed as follows :

$$t=\begin{Bmatrix} \tau_{rz}(r,z) \\ \sigma_{zz}(r,z) \\ \tau_{\theta z}(r,z) \end{Bmatrix} = \boldsymbol{J\kappa_2 eA} \quad \cdots\cdots(5)$$

where matrix κ_2 is defined by Eq. (A-2) in Appendix.

Since the unknown coefficients in vector A are determined from the boundary conditions, the displacement and the stress fields of Eqs.(3) and (5) can be expressed in terms of the unknown displacement and stress components at the lower interface of the layer. Moreover, the displacement and the stress components at the upper interface can be combined together and written in terms of the displacement and the stress components at the lower interface as follows:

$$\boldsymbol{Y_{j-1}=Ea_jE^{-1}Y_j} \quad \cdots\cdots(6)$$

where $E=diag\ (J, J)$

matrix $\boldsymbol{J}$ is shown in Eq.(4), transfer matrix $a_j=\kappa e^{-1}(d_j)\kappa^{-1}$, in which matrix $\kappa=[\kappa_1^T, \kappa_2^T]^T$, is defined by Eq.(A-3) in Appendix, $e(d_j)=e|_{z=d_j}, d_j$ is the thickness of the layer, and $\boldsymbol{Y_{j-1}}$ and $\boldsymbol{Y_j}$ are the unknown displacement-stress vectors at the upper and the lower interfaces of the layer, respectively.

Consider the total system shown in **Fig.1**. For a given layer in the system, Eq.(6) shows that the

displacement-stress vector at the upper interface can be expressed in terms of the displacement-stress vector at the lower interface. Therefore, by imposing the displacement and the stress continuity conditions at the horizontal interfaces from the first top layer down to the half-space layer, one can obtain the displacement-stress vector at the surface of the total system in terms of the displacement-stress vector at the surface of the half-space layer as expressed by Eq.(7).

$$\boldsymbol{Y}_0=\boldsymbol{E}\boldsymbol{a}_1\boldsymbol{a}_2\cdots\cdots\boldsymbol{a}_M\boldsymbol{E}^{-1}\boldsymbol{Y}_M=\boldsymbol{E}\boldsymbol{T}\boldsymbol{E}^{-1}\boldsymbol{Y}_M\cdots\cdots(7)$$

Consider the half-space layer in **Fig.1** alone. The general solution of the differential equations of wave propagation(Eqs.(2)) and the stress field in the half-space layer are similar to Eqs.(3) and (5) respectitively except that the upward propagating reflection wave must be suppressed. The displacement-stress vector at the surface of the half-space layer can then be written as

$$\boldsymbol{Y}_M=\begin{Bmatrix}u_M\\ t_M\end{Bmatrix}=\boldsymbol{E}\kappa'\boldsymbol{A}'\cdots\cdots(8)$$

where matrix $\kappa'=[\kappa_1'^T,\ \kappa_2'^T]^T$ in which the submatrices κ_1' and κ_2' are defined by Eqs(A-1a) and (A-2a) in Appendix respectively, and $\boldsymbol{A}'=(A_1,B_1,C_1)^T$ is the unknown vector determined from the boundary conditions at the surface of the half-space layer.

Eliminating $\boldsymbol{Y}_M$ in Eq.(7) using Eq.(8), Eq.(7) may be written as

$$\boldsymbol{Y}_0=\begin{Bmatrix}u_0\\ t_0\end{Bmatrix}=\begin{bmatrix}\boldsymbol{J}&0\\0&\boldsymbol{J}\end{bmatrix}\begin{bmatrix}\boldsymbol{T}_{11}&\boldsymbol{T}_{12}\\ \boldsymbol{T}_{21}&\boldsymbol{T}_{22}\end{bmatrix}\begin{bmatrix}\kappa_1'\\ \kappa_2'\end{bmatrix}\boldsymbol{A}'\cdots(9)$$

where $\boldsymbol{T}_{ij}'s$ are the submatrices of the matrix $\boldsymbol{T}$ in Eq.(7). After some matrix manpulations of eliminating the unknown vector $\boldsymbol{A}'$, one can obtain the displacement vector u_0 in terms of the stress vector t_0.

$$\begin{aligned}u_0&=\boldsymbol{J}(\boldsymbol{T}_{11}\kappa_1'+\boldsymbol{T}_{12}\kappa_2')(\boldsymbol{T}_{21}\kappa_1'+\boldsymbol{T}_{22}\kappa_2')^{-1}\boldsymbol{J}^{-1}t_0\\&=\boldsymbol{J}\boldsymbol{Q}\boldsymbol{J}^{-1}t_0\cdots\cdots(10)\end{aligned}$$

If the layered medium is assumed to be welded to a rigid lower boundary, then $u_M=0$ in $\boldsymbol{Y}_M$ in Eq.(7). This leads to $\boldsymbol{Q}=\boldsymbol{T}_{12}\boldsymbol{T}_{22}^{-1}$ for Eq.(10).

Equation (10) shows the relationship of the stress and the displacement vectors on the surface of the total system. However, it is very difficult to directly satisfy Eq.(10) with the arbitarily prescribed traction(Eq.(1)) acting on the surface. The prescribed traction thus must be properly decomposed first. A technique proposed in Ref.10) is used to decompose the prescribed traction in the following fashion.

Let $\bar{t}_0$ be the n^{th} Fourier component of the prescribed traction in Eq.(1). The traction $\bar{t}_0$ can be decomposed as follows[10] :

$$\begin{aligned}\bar{t}_0&=\begin{Bmatrix}\bar{\tau}_{rz}(r)\\ \bar{\sigma}_{zz}(r)\\ \bar{\tau}_{\theta z}(r)\end{Bmatrix}=\begin{Bmatrix}1\\0\\-1\end{Bmatrix}\frac{\bar{\tau}_{rz}(r)-\bar{\tau}_{\theta z}(r)}{2}\\&+\begin{Bmatrix}0\\1\\0\end{Bmatrix}\bar{\sigma}_{zz}(r)+\begin{Bmatrix}1\\0\\1\end{Bmatrix}\frac{\bar{\tau}_{rz}(r)+\bar{\tau}_{\theta z}}{2}\\&=\int_0^\infty\begin{Bmatrix}1\\0\\-1\end{Bmatrix}kJ_{n+1}(kr)\,C_{n+1}(k)\,dk\\&+\int_0^\infty\begin{Bmatrix}0\\1\\0\end{Bmatrix}kJ_n(kr)\,C_n(k)\,dk\\&+\int_0^\infty\begin{Bmatrix}1\\0\\1\end{Bmatrix}kJ_{n-1}(kr)\,C_{n-1}(k)\,dk\cdots\cdots(11)\end{aligned}$$

where

$$C_{n+1}(k)=\int_0^{a_0}r\frac{\bar{\tau}_{rz}(r)-\bar{\tau}_{\theta z}(r)}{2}J_{n+1}(kr)\,dr,\cdots\cdots(11a)$$

$$C_n(k)=\int_0^{a_0}r\,\bar{\sigma}_{zz}(r)J_n(kr)\,dr\cdots\cdots(11b)$$

and

$$C_{n-1}(k)=\int_0^{a_0}r\frac{\bar{\tau}_{rz}(r)+\bar{\tau}_{\theta z}(r)}{2}J_{n-1}(kr)\,dr\cdots\cdots(11c)$$

The integrals on the right hand sides of Eqs.(11) and (11a)—(11c) are Hankel transform pairs. Since the vector $(1,0,-1)^T$, $(0,1,0)^T$ and $(1,0,1)^T$ are orthogonal eigenvectors corresponding to the eigenvalues $-kJ_{n+1}(kr)$, $kJ_n(kr)$, and $kJ_{n-1}(kr)$ of the Bessel founction matrix J in Eq.(3)-(10), Eq.(11)can be rewritten as follows

$$\begin{aligned}\bar{t}_0&=\int_0^\infty-J\begin{Bmatrix}1\\0\\-1\end{Bmatrix}C_{n+1}(k)\,dk\\&+\int_0^\infty J\begin{Bmatrix}0\\1\\0\end{Bmatrix}C_n(k)\,dk+\int_0^\infty J\begin{Bmatrix}1\\0\\1\end{Bmatrix}C_{n-1}(k)\,dk\cdots\cdots(12)\end{aligned}$$

Since the continuity condition of the prescribed traction in Eq.(12) and the stress components on the surface of the total system in Eq.(10) must be satisfied ; i.e. $t_0=-\bar{t}_0$, one can obtain the dispalcement vector on the surface by substituting Eq.(12) into Eq.(10). This leads to the following equation.

$$u_0=\int_0^\infty \boldsymbol{JQ}\begin{Bmatrix}1\\0\\-1\end{Bmatrix}C_{n+1}(k)\,dk$$
$$-\int_0^\infty \boldsymbol{JQ}\begin{Bmatrix}0\\1\\0\end{Bmatrix}C_n(k)\,dk-\int_0^\infty \boldsymbol{JQ}\begin{Bmatrix}1\\0\\1\end{Bmatrix}C_{n-1}(k)\,dk$$
$$=\int_0^\infty \boldsymbol{JQ}\begin{Bmatrix}C_{n+1}(k)-C_{n-1}(k)\\C_n(k)\\-C_{n+1}(k)-C_{n-1}(k)\end{Bmatrix}dk \cdots\cdots (13)$$

Equation (13) concludes the analytic solution for the layered medium. Although Eq.(13) shows only the displacement components on the surface, the displacement and the stress fields in the layered medium can be determined in a similar fashion.

3. FORMULATION OF IMPEDANCE MATRIX

To generate impedance matrix using the analytic solution described in the preceding section, it is necessary to express the prescribed traction in a form compatible to finite element model of foundation structure. Therefore, the stress intensity in the r-direction of cylindrical coordinates for each Fourier component in Eq.(1) is assumed to be piecewise linear in the circular region with radius a_0 in **Fig.1**.

Assuming that the interval $(0, a_0)$ for Eq.(1) is divided into m subintervals with equal width $b=\frac{a_0}{m}$, one can express the piecewise linear stress distribution as follows :

$$\bar{\tau}_{rz}=\sum_{j=1}^{m-1}h_j(r)q_j+h_0(r)q_0+h_m(r)q_m=h^Tp$$
$$\bar{\sigma}_{zz}=\sum_{j=1}^{m-1}h_j(r)p_j+h_0(r)p_0+h_m(r)p_m=h^Tq$$
$$\bar{\tau}_{\theta z}=\sum_{j=1}^{m-1}h_j(r)s_j+h_0(r)s_0+h_m(r)s_m=h^Ts \cdots\cdots (14)$$

where

$$h_j(r)=\begin{cases}1+\frac{r-jb}{b}, & if\ (j-1)b\le r\le jb \text{ and } 1\le j\le m;\\ 1-\frac{r-jb}{b}, & if\ r\le (j+1)b \text{ and } 0\le j\le m-1;\\ 0, & \text{otherwise,}\end{cases} \cdots\cdots (14a)$$

and q_j, p_j and s_j are the stress intensities at node j for $\bar{\tau}_{rz}$, $\bar{\sigma}_{zz}$ and $\bar{\tau}_{\theta z}$ respectively.

Substituting Eqs.(14) into Eq.(11) and making use of Eq.(12), one can end up with the following equations.

$$\bar{t}_0=\begin{Bmatrix}\bar{\tau}_{rz}\\ \bar{\sigma}_{zz}\\ \bar{\tau}_{\theta z}\end{Bmatrix}$$
$$=\int_0^\infty J\begin{bmatrix}-D_{n+1}^T+D_{n-1}^T & 0 & D_{n+1}^T+D_{n-1}^T\\ 0 & D_n^T & 0\\ D_{n+1}^T+D_{n-1}^T & 0 & -D_{n+1}^T+D_{n-1}^T\end{bmatrix}\begin{Bmatrix}q\\p\\s\end{Bmatrix}dk=\int_0^\infty \boldsymbol{JDP}\,dk \cdots\cdots (15)$$

where

$$D_{n+1}^T=\int_0^{a_0}\frac{r}{2}J_{n+1}(kr)h^T\,dr,$$
$$D_n^T=\int_0^{a_0}rJ_n(kr)h^T\,dr \cdots\cdots (15a)$$

and

$$D_{n-1}^T=\int_0^{a_0}\frac{r}{2}J_{n-1}(kr)h^T\,dr$$

Using $t_0=-\bar{t}_0$ and substituting $t_0=-\boldsymbol{JDP}dk$ from Eq.(15) into Eq.(10), the following equation, which is equivalent to Eq.(13), can be obtained by integrating the resulting expression from 0 to ∞.

$$u_0=-\int_0^\infty \boldsymbol{JQDP}\,dk \cdots\cdots (16)$$

Equation (16) defines the relationship between the displacement vector and the prescribed traction on the surface for the n^{th} Fourier component. To generate the impedance matrix, one can use the substructuring concept, the principle of virtual work, and the reciprocal theorem. Employing the orthogonal property of Fourier series, only one Fourier component is considered in the following formulations.

Consider the layered medium with the prescribed traction defined by Eq.(14). Applying the variational principle to the system, one may have the equations as follows :

$$\delta W=\int_0^{a_0}\int_0^{2\pi}\delta\,\bar{t}_0^T u_0 r\,d\theta\,dr$$
$$=-\begin{pmatrix}2\pi\\ \pi\end{pmatrix}\delta\boldsymbol{P}^T\int_0^{a_0}\boldsymbol{H}\int_0^\infty \boldsymbol{JQD}\,dk\,dr\boldsymbol{P}$$
$$=-\begin{pmatrix}2\pi\\ \pi\end{pmatrix}\delta\boldsymbol{P}^T\int_0^\infty\left(\int_0^{a_0}\boldsymbol{HJ}r\,dr\right)\boldsymbol{QD}\,dk\boldsymbol{P} \cdots\cdots (17)$$

where $H=diag\ (h, h, h)$,
and h, $\bar{t}_0$ and u_0 are defined in Eqs.(10) and (12) respectively. The coefficients 2π and π in Eq.(17) come from the integrals $\int_0^{2\pi}\cos^2 n\theta\,d\theta$ or

$\int_0^{2\pi} \sin^2 n\theta d\theta$ which are not explicitly expressed in the formulations. Furthermore, using the procedure developed to obtain Eq.(15), one can show that

$$\int_0^{a_0} HJrdr = kD^T \quad \cdots\cdots (18)$$

where the matrix $\boldsymbol{D}$ is defined in Eq.(15). The virtual work in Eq.(17) can then be rewriteen in the form as follows:

$$\delta W = -\begin{pmatrix} 2\pi \\ \pi \end{pmatrix} \delta \boldsymbol{P}^T \int_0^{\infty} \boldsymbol{D}^T \boldsymbol{Q} \boldsymbol{D} k dk \boldsymbol{P}$$

$$= \begin{pmatrix} 2\pi \\ \pi \end{pmatrix} \delta \boldsymbol{P}^T \boldsymbol{K} \boldsymbol{P} \quad \cdots\cdots (19)$$

Using Eq.(10) and Betti's Theorem, one can show that the matrix $\boldsymbol{Q}$ is symmetric. Therefore, the matrix $\boldsymbol{K} = -\int_0^{\infty} \boldsymbol{D}^T \boldsymbol{Q} \boldsymbol{D} k dk$ is also symmetric.

Now, consider the foundation itself. Similar to the finite element modelling, the diplacement field of the foundation for the n^{th} Fourier component can be assumed as :

$$\bar{u}_0 = \boldsymbol{N} v \begin{pmatrix} \cos n\theta \\ \sin n\theta \end{pmatrix} \quad \cdots\cdots (20)$$

where matrix $\boldsymbol{N}$ is comprised of the shape function in the r-direction, and vector v is comprised of the generalized displacements at the nodal rings of the foundation finite element model. Similarly, the virtual work of the system is obtained by applying the variational principle

$$\delta W = \int_0^{2\pi} \int_0^{a_0} \delta \bar{t}_0^T \bar{u}_0 r dr d\theta$$

$$= \begin{pmatrix} 2\pi \\ \pi \end{pmatrix} \delta \boldsymbol{P}^T \int_0^{a_0} \boldsymbol{H} \boldsymbol{N} r dr v$$

$$= \begin{pmatrix} 2\pi \\ \pi \end{pmatrix} \delta \boldsymbol{P}^T B v \quad \cdots\cdots (21)$$

Equating Eq.(21) to Eq.(19) and factoring out $\delta \boldsymbol{P}^T$, it is obtaned

$$\begin{pmatrix} 2\pi \\ \pi \end{pmatrix} \boldsymbol{K} \boldsymbol{P} = \begin{pmatrix} 2\pi \\ \pi \end{pmatrix} B v \quad \cdots\cdots (22)$$

or

$$\boldsymbol{V} = \begin{pmatrix} 2\pi \\ \pi \end{pmatrix} B v \quad \cdots\cdots (22a)$$

where vector $\boldsymbol{V}$ are the generalized displacements at the nodal rings of the assumed piecewise linear stress model. Eq.(22a) gives the relationship between the nodal generalized displacements of the assumed stress model of Eqs.(14) and the finite element model of Eq.(20). To obtaing the corresponding force-stress relationship for both models, the reciprocal theorem can be used. This leads to the following equation.

$$\boldsymbol{F} = \begin{pmatrix} 2\pi \\ \pi \end{pmatrix} \boldsymbol{B}^T \boldsymbol{P} \quad \cdots\cdots (23)$$

where vector $\boldsymbol{F}$ are the generalized forces at the nodal rings of the finite element model. Substituting $\boldsymbol{P} = \boldsymbol{K}^{-1} B v$ from Eq.(22) into Eq.(23) yields

$$\boldsymbol{F} = \begin{pmatrix} 2\pi \\ \pi \end{pmatrix} \boldsymbol{B}^T \boldsymbol{K}^{-1} B v = \boldsymbol{I} v \quad \cdots\cdots (24)$$

The matrix $\boldsymbol{I}$ is the impedance matrix for the n^{th} Fourier component. After the impedance matrices for all the necessary Fourier components are determined, the analysis of soil-structure interaction can then be carried out by incorporating these impedance matrices into the total stiffness matrix of the system. Again, it is noted that both matrices $\boldsymbol{I}$ and $\boldsymbol{K}$ in Eq.(24) are symmetric.

4. NUMERICAL ANALYSES

In the semi-infinite integration of Eq.(19), singular points may exist provided there is no damping assumed for the soil medium. Although technique such as residue theorem may be used to calculate the integrations around the singular points, material damping is assumed in the soil medium in order to comply with the more realistic situation of soil medium. Also, the branch cuts due to multivalued functions ν and ν' move away from the integration path of Eq.(19), if damping is introduced in the medium. Therefore, numerical integration scheme can be directly employed. A. 05 hysteretic damping ratio is chosen in the following numerical examples and the Poisson ratio of the soil medium is assumed to be $\frac{1}{3}$. Furthermore, using the following two statements, the integrand in the semi-infinite integral can be easily shown to be proportional to $\frac{1}{k^3}$ as $k \to \infty$:

(1) The elements of matrix Q decay with $\frac{1}{k}$ as $k \to \infty$, since only downward propagating waves need to be considered and $\nu \doteq \nu' \doteq k$.

(2) Using the identities of $\int r^2 J_n(kr) dr = -\frac{r^2}{k} J_{n+1}(kr) + \frac{n+1}{k} \int r J_{n-1}(kr) dr$ and $\int r J_n(kr) dr = -\frac{r}{k} J_{n-1}(kr) + \frac{n}{k} \int J_{n-1}(kr) dr$, and $J_n(kr) \propto \frac{1}{k^{0.5}}$ as $\to \infty$, it is concluded that the elements of matrix $\boldsymbol{D}$ in

Table 1 Nondimensionalized Torsional Impedance

	Nondimensional Frequency $\frac{\omega a_o}{Re(c_s)} = 9.8960$					
	$m = 10$		$m = 20$		$m = 50$	
$k_{max}a_o$ = 170.	$ng = 3$	$4.3147 + 14.4484i$	$ng = 3$	$3.9052 + 15.1328i$	$ng = 3$	$3.9429 + 15.2932i$
	$ng = 5$	$3.8416 + 14.9466i$	$ng = 5$	$3.9016 + 15.1207i$	$ng = 5$	$3.9428 + 15.2929i$
$k_{max}a_o$ = 395.	$ng = 9$	$4.0027 + 14.8617i$	$ng = 5$	$3.9549 + 15.0655i$	$ng = 3$	$3.9429 + 15.2932i$
	$ng = 12$	$3.8422 + 14.9497i$	$ng = 7$	$3.8987 + 15.0996i$	$ng = 5$	$3.9428 + 15.2929i$
$k_{max}a_o$ = 1145.	-	—	$ng = 16$	$3.8987 + 15.0952i$	-	—
	-	—	$ng = 20$	$3.8981 + 15.0955i$	-	—

Table 2 Nondimensionalized Vertical Impedance

	Nondimensional Frequency $\frac{\omega a_o}{Re(c_s)} = 9.8960$					
	$m = 10$		$m = 20$		$m = 50$	
$k_{max}a_o$ = 170.	$ng = 3$	$10.0944 + 59.5764i$	$ng = 3$	$6.9536 + 61.2884i$	$ng = 3$	$6.9924 + 61.6245i$
	$ng = 5$	$6.8594 + 60.8990i$	$ng = 5$	$6.9447 + 61.2625i$	$ng = 5$	$6.9923 + 61.6239i$
$k_{max}a_o$ = 395.	$ng = 9$	$7.8845 + 60.6744i$	$ng = 5$	$7.3067 + 61.1330i$	$ng = 3$	$6.9814 + 61.4255i$
	$ng = 12$	$6.8582 + 60.9082i$	$ng = 7$	$6.9443 + 61.2187i$	$ng = 5$	$6.9780 + 61.4175i$
$k_{max}a_o$ = 595.	-	—	$ng = 7$	$7.0380 + 61.1808i$	$ng = 3$	$6.9795 + 61.4152i$
	-	—	$ng = 9$	$6.9438 + 61.2135i$	$ng = 5$	$6.9773 + 61.4062i$

Table 3 Nondimensionalized Torsional Impedance

	Nondimensional Frequency $\frac{\omega a_o}{Re(c_s)} = 5.1836$					
	$m = 10$		$m = 20$		$m = 50$	
$k_{max}a_o$ = 170.	$ng = 3$	$3.6142 + 7.2902i$	$ng = 3$	$3.6096 + 7.6210i$	$ng = 3$	$3.6425 + 7.7082i$
	$ng = 5$	$3.5688 + 7.5272i$	$ng = 5$	$3.6071 + 7.6151i$	$ng = 5$	$3.6424 + 7.7080i$
$k_{max}a_o$ = 395.	$ng = 9$	$3.5950 + 7.4865i$	$ng = 5$	$3.6118 + 7.5870i$	$ng = 3$	$3.6238 + 7.6546i$
	$ng = 12$	$3.5691 + 7.5281i$	$ng = 7$	$3.6034 + 7.6038i$	$ng = 5$	$3.6230 + 7.6527i$
$k_{max}a_o$ = 595.	-	—	$ng = 7$	$3.6044 + 7.5958i$	$ng = 3$	$3.6228 + 7.6523i$
	-	—	$ng = 9$	$3.6030 + 7.6026i$	$ng = 5$	$3.6220 + 7.6499i$

Eq.(19) decay with $\frac{1}{k^{1.5}}$.

It is therefore appropriate to replace the infinite integration limit with a finite number without lossing precision.

The accuracy in calculating the impedance matrix or functions using the preceding procedure is dependent upon the integration schemes used for calculating the matrices $\boldsymbol{D}$ in Eq.(15) and $\boldsymbol{K}$ in Eq.(19), and the number of subintervals used for the stress model in Eq.(14). A numerical study is designed to address these concerns. In this study, the total system is a rigid circular plate welded on a half-space medium and subjected to torsional and vertical harmonic excitations. Some of the numerical results are shown in **Table 1~6**. In the tables, m is the number of subintervals for the stress model in Eq.(14), ng is the number of the integration points for Gaussian quadrature used to calculate the elements in the matrix $\boldsymbol{D}$ of Eq.(15a), and $k_{\max}$ is the number used to replace the infinite integration limit in Eq.(19). One should also notice that all the numerical results in the tables and the following figures have been nondimensionalized.

Since sharp variations often occur to the integrand of the semi-infinite integral in Eq.(19) in the region between 0 and Rayleigh surface wave number, which is smaller than $\frac{1.16\omega}{Re(c_s)}$, the entire integration range is divided into two regions, namely $0 \sim \frac{1.5\omega}{Re(c_s)}$ and $\frac{1.5\omega}{Re(c_s)} \sim k_{\max}$, in which c_s is the complex shear wave velocity of the half-space medium. The reason to choose $\frac{1.5\omega}{Re(c_s)}$ as dividing point for integration is to ensure that the accuracy of the integration in the region with sharp variations is maintained. For the integration in the first region, small intervals and high order integration formula of Gaussian quadrature(60 equal intervals and 20-point formula) are used. In the second region, the integration intervals become larger and larger as k increases. For larger k, the sizes of integration intervals may be also controlled by the degree of the variation of Bessel function $J_n(kr)$.

In general, a larger number of subintervals for the stress model in Eq.(14) is necessary for higher frequencies, if the same degree of accuracy is desired for the entire range of desired frequencies. After examining the tables, however, it can be fairly said that, in terms of precision for impedances, 20 linear stress subintervals are sufficient for the entire range of the nondimensional frequencies $0 \sim 10.0$.

The impedances by increasing $k_{\max}$ and m, as shown in the tables, are converging, and it is also

Table 4 Nondimensionalized Vertical Impedance

	Nondimensional Frequency $\frac{\omega a_0}{Re(c_s)} = 5.1836$					
	$m = 10$		$m = 20$		$m = 50$	
$k_{max}a_0$ = 170.	$ng = 3$	6.5698 + 31.6571i	$ng = 3$	5.7959 + 32.4121i	$ng = 3$	5.8256 + 32.5933i
	$ng = 5$	5.7511 + 32.2170i	$ng = 5$	5.7922 + 32.3994i	$ng = 5$	5.8255 + 32.5930i
$k_{max}a_0$ = 395.	$ng = 9$	6.0139 + 32.1224i	$ng = 5$	5.8817 + 32.3372i	$ng = 3$	5.8105 + 32.4816i
	$ng = 12$	5.7510 + 32.2196i	$ng = 7$	5.7896 + 32.3761i	$ng = 5$	5.8092 + 32.4776i
$k_{max}a_0$ = 595.	-	—	$ng = 7$	5.8126 + 32.3583i	$ng = 3$	5.8095 + 32.4765i
	-	—	$ng = 9$	5.7892 + 32.3734i	$ng = 5$	5.8084 + 32.4717i

Table 5 Nondimensionalized Torsional Impedance

	Nondimensional Frequency $\frac{\omega a_0}{Re(c_s)} = 0.1571$					
	$m = 10$		$m = 20$		$m = 50$	
$k_{max}a_0$ = 170.	$ng = 3$	5.1051 + 0.0048i	$ng = 3$	5.2797 + 0.0052i	$ng = 3$	5.3278 + 0.0052i
	$ng = 5$	5.2325 + 0.0051i	$ng = 5$	5.2769 + 0.0051i	$ng = 5$	5.3277 + 0.0052i
$k_{max}a_0$ = 395.	$ng = 9$	5.2090 + 0.0050i	$ng = 5$	5.2613 + 0.0051i	$ng = 3$	5.2967 + 0.0052i
	$ng = 12$	5.2325 + 0.0051i	$ng = 7$	5.2710 + 0.0051i	$ng = 5$	5.2958 + 0.0052i
$k_{max}a_0$ = 595.	-	—	$ng = 7$	5.2667 + 0.0051i	$ng = 3$	5.2955 + 0.0052i
	-	—	$ng = 9$	5.2703 + 0.0051i	$ng = 5$	5.2943 + 0.0052i

Table 6 Nondimensionalized Vertical Impedance

	Nondimensional Frequency $\frac{\omega a_0}{Re(c_s)} = 0.1571$					
	$m = 10$		$m = 20$		$m = 50$	
$k_{max}a_0$ = 170.	$ng = 3$	5.9704 + 0.7753i	$ng = 3$	6.0497 + 0.7960i	$ng = 3$	6.0680 + 0.8008i
	$ng = 5$	6.0315 + 0.7912i	$ng = 5$	6.0486 + 0.7957i	$ng = 5$	6.0680 + 0.8008i
$k_{max}a_0$ = 395.	$ng = 9$	6.0192 + 0.7880i	$ng = 5$	6.0413 + 0.7938i	$ng = 3$	6.0562 + 0.7977i
	$ng = 12$	6.0315 + 0.7912i	$ng = 7$	6.0463 + 0.7951i	$ng = 5$	6.0559 + 0.7976i
$k_{max}a_0$ = 595.	-	—	$ng = 7$	6.0443 + 0.7945i	$ng = 3$	6.0557 + 0.7976i
	-	—	$ng = 9$	6.0460 + 0.7950i	$ng = 5$	6.0553 + 0.7974i

observed that $k_{max}a_0=170$, in which a_0 is the radius of the circular plate, is enough to give accurate results over the nondimensional frequency range 0 ~10.0. Since Bessel function $J_n(kr)$ varies more sharply in the r-direction as k increases, the number of integration points in calculating the elements in the matrix $\boldsymbol{D}$ in Eq.(15a) must be increased either as k_{max} increases, or as the number of subintervals for the stress model decreases. According to the tables, $ng=3$ can give accurate results, if $k_{max}a_0=170$ and $m=20$.

Therefore, $m=20$, $k_{max}a_0=170$ and $ng=3$ are chosen in the following example to investigate the influences of layered stratum on the impedance functions. **Fig.2** shows the total system of the example, which is a rigid massless circular plate rigidly attached to a two-layer system and subjected to torsional, vertical, rocking and horizontal vibrations. The corresponding impedances are defined as follows :

K_{TT} is the torsional impedance, K_{VV} is the vertical impedance, K_{RR} is the rocking impedance, $K_{RH}=K_{HR}$ are the coupling impedances for rocking and horizontal motions, and K_{HH} is the horizontal impedance. The numerical results of these impedances are shown in **Fig.3**~8.

In order to demonstrate the presented method further, **Fig.3** compares the vertical impedance K_{VV} with the corresponding result in reference[7] for the case of half space medium[7]. In the figure, one can observe both results agree to each other. Also, one may not distinguish the result with welded condition from that with relaxed condition (neglecting contact shear stress). The result with welded

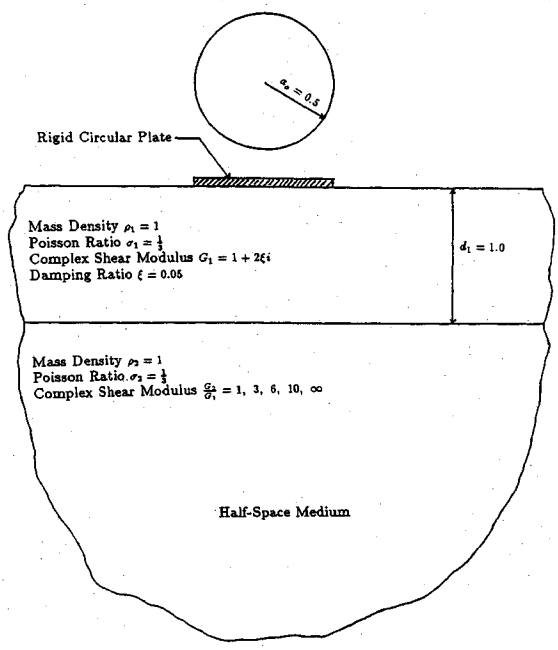

Fig.2 Soil Profile of Example.

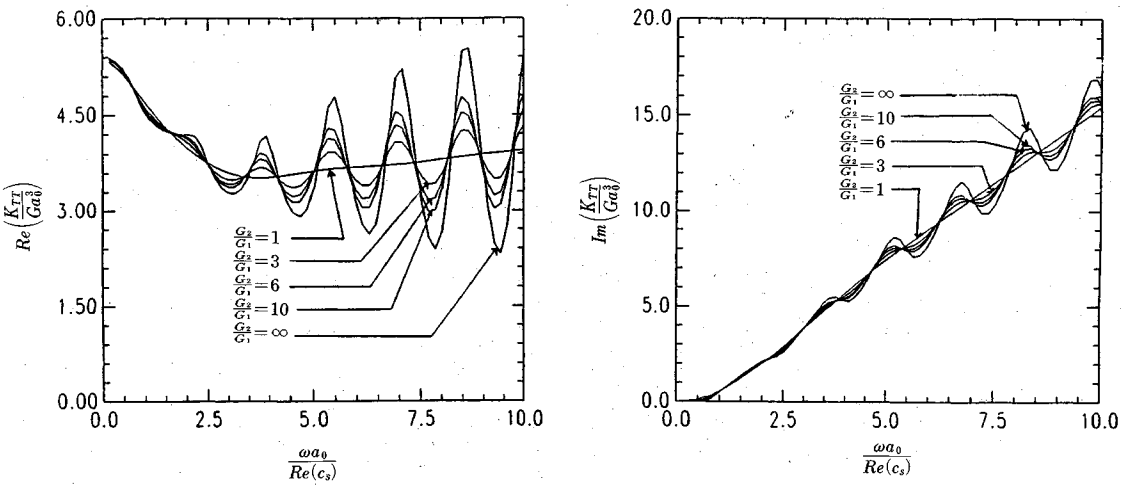

Fig.4 Nondimensionalized Torsional Impedance.

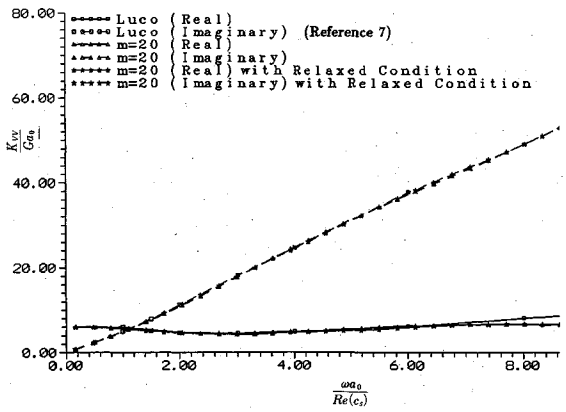

Fig.3 Comparison of Vertical Impedance.

condition actually is slightly higher than that with relaxed condition.

From **Fig.4**~8, one can see that the impedance functions for the layered system fluctuate along the corresponding impedance functions for the half-space medium, and the fluctuations become more dramatic as the lower half-space layer goes stiffer. This phenomenon can be explained as the influence of the reflection waves from the horizontal interface of the two-layer system. The reflection waves can be either amplifying or diminishing, which are dependent upon the excitation frequency, the responeses at the surface.

For the case of torsional excitation, only shear waves are involved in the formulation of impedance function. Therefore, the nondimensional frequency difference between two adjacent peaks in **Fig.4** is about $\frac{\pi}{2}$. This is identical to the characteristic behavior of propagating shear waves in the top layer of the two-layer system. For the case of vertical excitation, all the shear, compressional and Rayleigh surface waves are involved, and these waves have effects to each other. The behavior of the impedance function (**Fig.5**), thus, has more irregularities. However, by observing the nondimensional frequency differences between two adjacent peaks in **Fig.5**, one can conclude that compressional waves and Rayleigh surface waves govern the behavior of the impedance function for the case of layered medium. By comparing the horizontal impedance function in **Fig.6** to the torsional impedance function in **Fig.4**, one can observe some similarities. This demonstrates that shear waves dominate in the case of horizontal excitation. Whereas, compressional and Rayleigh surface waves are more important in the case of rocking excitation. This can be concluded by comparing **Fig.8** to **Fig.5**. The coupling impedance, shown in **Fig.7**, may be small for the case of half space medium. However, it is not true for the case of layered medium. This suggests that the coupling impedance can not be ignored in the analysis of soil-structure interaction.

Fig.9 show the typical distribution of nondimensionalized contact normal stress for the vertical vibration of the rigid circular plate on half space medium. In the figure, one can observe that curves for $m=20$ and $m=40$ respectively are almost identical for $r\leq 0.47$. For $r\geq 0.47$ the curves do not match well to each other. This is because the stress should go infinite as $r\rightarrow a_0(a_0=0.5)$. This suggests that the subintervals for the stress model of Eq.(14) should be small enough near the edge of the plate, if one wants to calculate the contact stresses more correctly at the edge. However, this inaccuracy only has little effect on the accuracy of

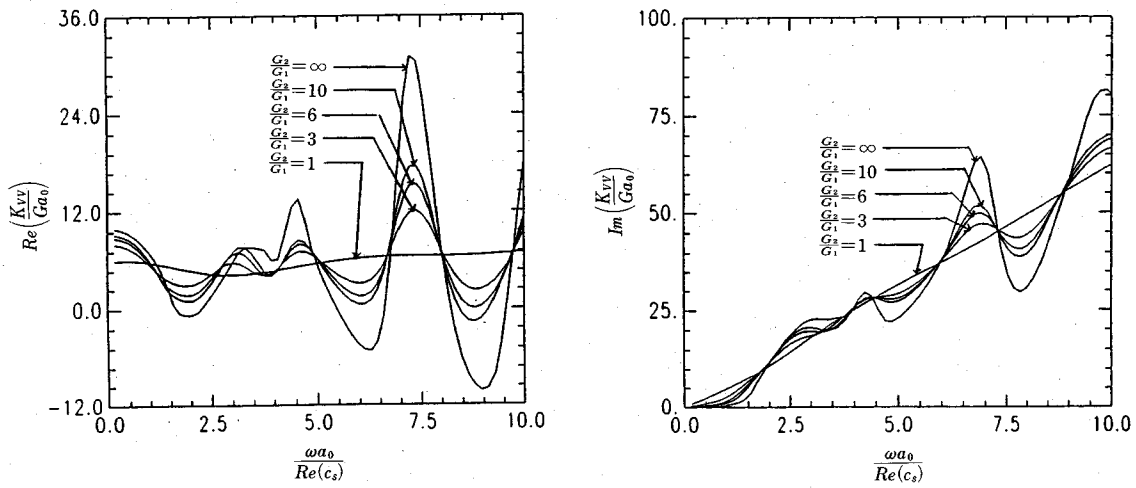

Fig.5 Nondimensionalized Vertical Impedance.

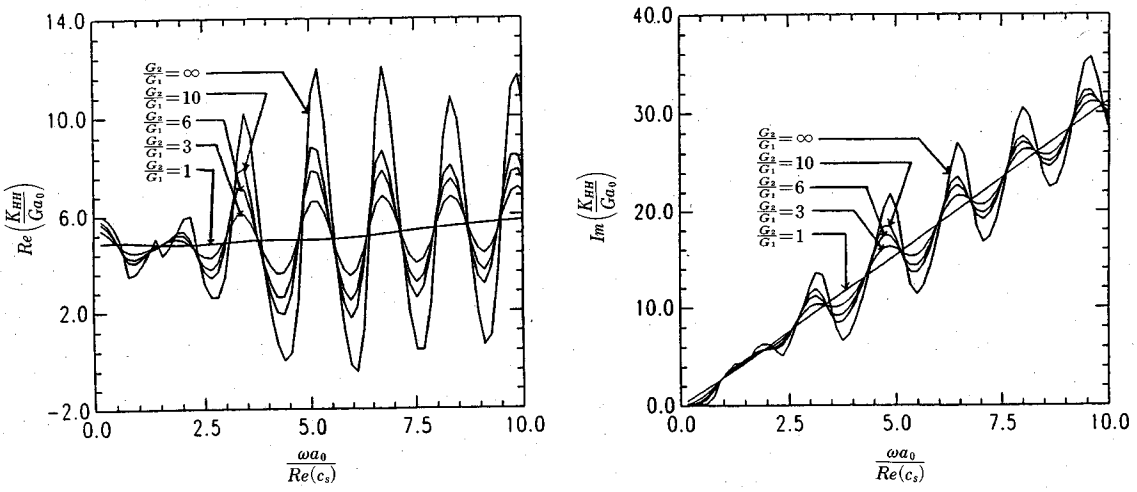

Fig.6 Nondimensionalized Horizontal Impedance.

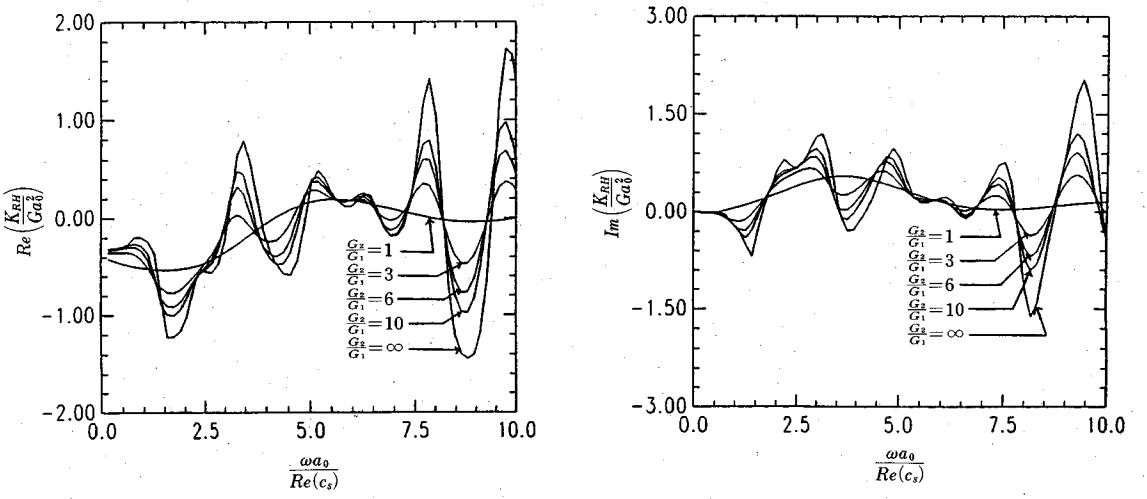

Fig.7 Nondimensionalized Coupling Impedance.

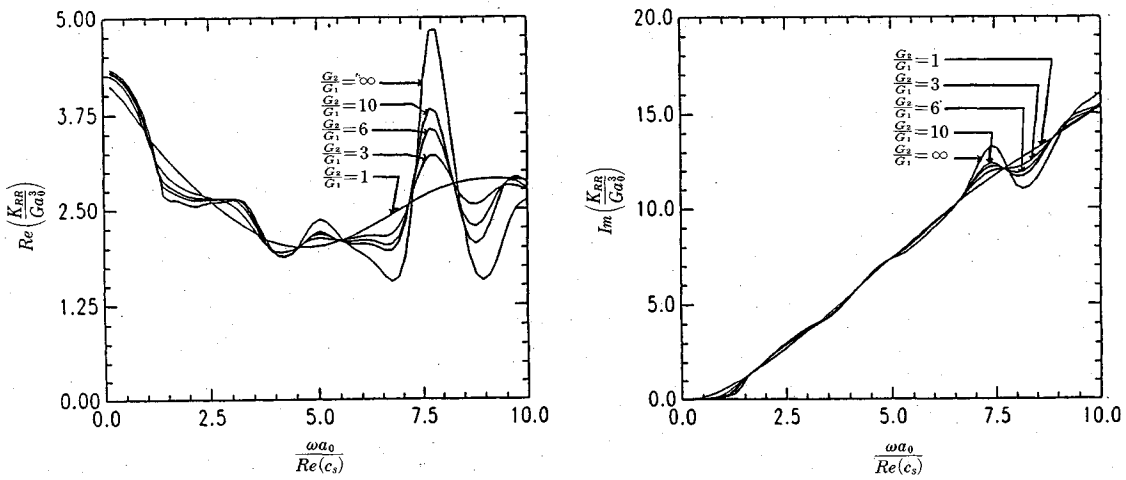

Fig.8 Nondimensionalized Rocking Impedance.

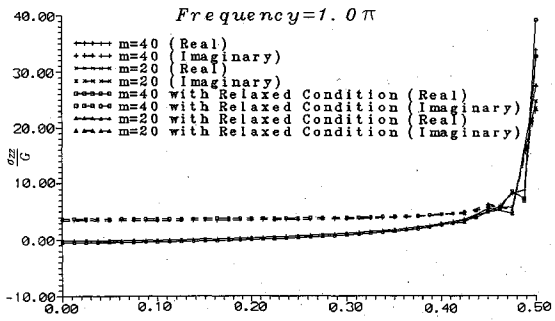

Fig.9 Typical Distribution of Contact Normal Stress ($\omega=1.0\pi$).

impedances.

ACKNOWLEDGEMENTS

The financial support of this research is partly provided by National Science Council of Taiwan through Contract No. 80-0410-E-009-03.

APPENDIX

The matrix κ_1 in Eq.(3) is expressed as follows :

$$\kappa_1=[\kappa_1' \quad \kappa_1''] \cdots\cdots (A\text{-}1)$$

where

$$\kappa_1'=\begin{bmatrix} k & -\nu_j' & 0 \\ -\nu_j & k & 0 \\ 0 & 0 & 1 \end{bmatrix} \cdots\cdots (A\text{-}1a)$$

and

$$\kappa_1''=\begin{bmatrix} k & \nu_j' & 0 \\ \nu_j & k & 0 \\ 0 & 0 & 1 \end{bmatrix} \cdots\cdots (A\text{-}1b)$$

The matrix κ_2 in Eq.(5) is expressed as follows :

$$\kappa_2=[\kappa_2' \quad \kappa_2''] \cdots\cdots (A\text{-}2)$$

where

$$\kappa_2'=\begin{bmatrix} -2kG_j\nu_j & G_j(2k^2-k_{\beta_j}^2) & 0 \\ G_j(2k^2-k_{\beta_j}^2) & -2kG_j\nu_j' & 0 \\ 0 & 0 & -G_j\nu_j' \end{bmatrix} \cdots\cdots (A\text{-}2a)$$

and

$$\kappa_2''=\begin{bmatrix} 2kG_j\nu_j & G_j(2k^2-k_{\beta_j}^2) & 0 \\ G_j(2k^2-k_{\beta_j}^2) & 2kG_j\nu_j' & 0 \\ 0 & 0 & G_j\nu_j' \end{bmatrix} \cdots\cdots (A\text{-}2b)$$

in which $k_{\beta_j}^2=\dfrac{\omega^2}{c_{gj}^2}$.

The transfer matrix a_j in Eq.(6) is expressed as follows :

$$a_j=\begin{bmatrix} a_{11} & a_{12} \\ a_{21} & a_{22} \end{bmatrix} \cdots\cdots (A\text{-}3)$$

where

$$a_{11}=\begin{bmatrix} \dfrac{2k^2}{k_{\beta_j}^2}(CH-CH')+CH' & \dfrac{k}{k_{\beta_j}^2}\left((2k^2-k_{\beta_j}^2)\dfrac{SH}{\nu_j}-2\nu_j'SH'\right) & 0 \\ \dfrac{k}{k_{\beta_j}^2}\left(-2\nu_jSH+(2k^2-k_{\beta_j}^2)\dfrac{SH'}{\nu_j'}\right) & CH-\dfrac{2k^2}{k_{\beta_j}^2}(CH-CH') & 0 \\ 0 & 0 & CH' \end{bmatrix}, \cdots\cdots (A\text{-}3a)$$

$$a_{12}=\begin{bmatrix} \frac{1}{G_j k_{\beta_j}^2}\left(\nu_j' SH' - k^2 \frac{SH}{\nu_j}\right) & \frac{-k}{G_j k_{\beta_j}^2}(CH-CH') & 0 \\ \frac{k}{G_j k_{\beta_j}^2}(CH-CH') & \frac{1}{G_j k_{\beta_j}^2}\left(\nu_j SH - k^2 \frac{SH'}{\nu_j'}\right) & 0 \\ 0 & 0 & -\frac{SH'}{G_j \nu_j'} \end{bmatrix} \quad \cdots\cdots\text{(A-3b)}$$

$$a_{21}=\begin{bmatrix} G_j\left(\frac{-4k^2}{k_{\beta_j}^2}\nu_j SH + \frac{(2k^2-k_{\beta_j}^2)^2}{k_{\beta_j}^2}\frac{SH'}{\nu_j'}\right) & \frac{-2kG_j}{k_{\beta_j}^2}(2k^2-k_{\beta_j}^2)(CH-CH') & 0 \\ \frac{2kG_j}{k_{\beta_j}^2}(2k^2-k_{\beta_j}^2)(CH-CH') & G_j\left(\frac{(2k^2-k_{\beta_j}^2)^2}{k_{\beta_j}^2}\frac{SH}{\nu_j} - \frac{4k^2}{k_{\beta_j}^2}\nu_j' SH'\right) & 0 \\ 0 & 0 & -G_j \nu_j' SH' \end{bmatrix} \quad \cdots\cdots\text{(A-3c)}$$

and

$$a_{22}=\begin{bmatrix} \frac{2k^2}{k_{\beta_j}^2}(CH-CH')+CH' & \frac{k}{k_{\beta_j}^2}\left(2\nu_j' SH' - (2k^2-k_{\beta_j}^2)\frac{SH}{\nu_j}\right) & 0 \\ \frac{k}{k_{\beta_j}^2}\left(2\nu_j SH - (2k^2-k_{\beta_j}^2)\frac{SH'}{\nu_j'}\right) & CH - \frac{2k^2}{k_{\beta_j}^2}(CH-CH') & 0 \\ 0 & 0 & CH' \end{bmatrix} \quad \cdots\cdots\text{(A-3d)}$$

in which $SH=\sin h\nu_j d_j$, $SH'=\sin h\nu_j' d_j$, $CH=\cos h\nu_j d_j$ and $CH'=\cos h\nu_j' d_j$.

REFERENCES

1) Waas, G. : Linear Two-Dimensional Analysis of Soil Dynamic Problems in Semi-Infinite Layered Media, Ph. D. Dissertation, UC Berkeley, CA, 1972.
2) Kausel, E. : Forced Vibrations of Circular Foundations on Layered Media, R 74-11, Dept. of Civil Eng., MIT, Jan. 1974.
3) Apsel, R.J. and Luco, J.E. : Impedance Functions for Foundations Embeded in A Layered Medium : An Integral Equation Approach, Earthquake Eng. Str. Dyn., Vol 15, 213~231, 1987.
4) Wolf, J.P. and Darbre, G.R. : Dynamic Stiffness Matrix of Soil by Boundary Element Method : Conceptual Aspects, Earthquake Eng. Str. Dyn., Vol 12, 385~400, 1984.
5) Lysmer, J. : Vertical Motion of Rigid Footings'Ceport No. 3-115, Dept. of Civil Eng., U. of Michigan, 1965.
6) Luco, J.E. and Westmann, R.A. : Dynamic Response of Circular Footings, J. Eng. Mech., ASCE, Vol 97, EM 5, Oct. 1971.
7) Luco, J.E. : Impedance Functions for A Foundation on A Layered Medium, Nuclear Eng. Design, 31, 204~217, 1974.
8) Luco, J.E. : Vibrations of A Rigid Disc on A Layered Viscoelastic Medium, Nuclear Eng. Design, 36, 325~340, 1976.
9) Wong, H.L. and Luco, J.E. : Dynamic Response of Regid Foundations of Arbitary Shape, Earthquake Eng. Str. Dyn., Vol. 4, 579~587, 1976.
10) Liou, G.S. : Analytic Solution for Soil-Structure Interaction in Layered Media, Earthquake Eng. Str. Dyn., Vol.18, 667~686, 1989.
11) Sezawa, K. : Further Studies on Rayleigh Waves Having Some Azimuthal Distribution, B. Earthquake Res. Inst., Vol. 6, 1~18, 1929.

(Received October 12. 1990)